Plant Physiology®

Plant Physiology, 2025, **198**, kiaf196
https://doi.org/10.1093/plphys/kiaf196
Advance access publication 9 May 2025
Research Article

Role of polar localization of the silicon transporter OsLsi1 in metalloid uptake by rice roots

Noriyuki Konishi, Namiki Mitani-Ueno, Jian Feng Ma*

Institute of Plant Science and Resources, Okayama University, Kurashiki 710-0046, Japan
*Author for correspondence: maj@rib.okayama-u.ac.jp
The author responsible for distribution of materials integral to the findings presented in this article in accordance with the policy described in the Instructions for Authors (https://academic.oup.com/plphys/pages/General-Instructions) is: Jian Feng Ma (maj@rib.okayama-u.ac.jp).

Abstract

Low silicon (Si) rice 1 (OsLsi1) is a key transporter mediating Si uptake in rice (*Oryza sativa*). It is polarly localized at the distal side of the root exodermis and endodermis. Although OsLsi1 is also permeable to other metalloids, such as boron (B), germanium (Ge), arsenic (As), antimony (Sb), and selenium (Se), the role of its polar localization in the uptake of these metalloids remains unclear. In this study, we investigated the role of OsLsi1 polar localization in metalloid uptake by examining transgenic rice plants expressing polarly or nonpolarly localized OsLsi1 variants. Loss of OsLsi1 polar localization resulted in decreased accumulation of Ge, B, and As in shoots but increased Sb accumulation, while Se accumulation remained unaffected under normal conditions. Experiments with varying B concentrations revealed that B uptake is significantly lower at low B concentrations (0.3 to 3 μM) but higher at high B concentrations (300 μM) in plants expressing nonpolarly localized OsLsi1, despite the similar B permeability of both OsLsi1 variants in *Xenopus* oocytes and their comparable protein abundance in roots. Additionally, the loss of OsLsi1 polarity did not affect the abundance, localization, or high B-induced degradation of the borate transporter 1 (OsBOR1), an efflux transporter that cooperates with OsLsi1 for B uptake. Taken together, our findings demonstrate that the polar localization of OsLsi1 plays a critical role in regulating metalloid uptake, depending on the presence or absence of efflux transporters cooperating with OsLsi1.

Introduction

Uptake of mineral nutrients by plant roots from the soil solution relies on various transporters (Che et al. 2018; Huang et al. 2020, 2024a; Rengel et al. 2022). So far, a number of transporters for different elements have been identified in different plant species, and some of them have been reported to show polar localization (Gordon-Weeks et al. 2003; Ma et al. 2006, 2007; Ueno et al. 2009, 2015; Takano et al. 2010; Kiba et al. 2012; Sasaki et al. 2012; Barberon et al. 2014; Konishi and Ma 2021; Guo et al. 2022; Huang et al. 2022). For example, 2 transporters for boron (B) uptake in Arabidopsis, Nodulin 26-like Intrinsic Protein (NIP) 5;1 (AtNIP5;1) and borate transporter 1 (AtBOR1), show polar localization in the roots. AtNIP5;1 is localized at the distal side of the epidermis and endodermis, while AtBOR1 is localized at the proximal side of the epidermis and endodermis (Yoshinari et al. 2016; Wang et al. 2017). A NITRATE TRANSPORTER2.4 (Kiba et al. 2012) and an iron transporter IRON-REGULATED TRANSPORTER 1 (AtIRT1) (Barberon et al. 2014) in Arabidopsis are also reported to show polar localization at the distal side in the root epidermal cells. In addition, phosphate transporters (PTs), including StPT2 in potatoes (Gordon-Weeks et al. 2003) and GmPT4 in soybean (Guo et al. 2022), and a transporter YELLOW STRIPE 1 (ZmYS1) for ferric–mugineic acid complex in maize (Ueno et al. 2009) were also reported to be localized at the distal side of root epidermal cells.

In rice, several transporters for the uptake of mineral elements show polar localization. Low silicon (Si) rice 1 (OsLsi1) and OsLsi2 required for Si uptake are polarly localized at the distal and proximal sides, respectively, of both exodermis and endodermis in the root mature region (Ma et al. 2006, 2007). Similarly, OsBOR1 responsible for B uptake and 2 transporters, NATURAL RESISTANCE-ASSOCIATED MACROPHAGE PROTEIN 5 (OsNramp5) and METAL TOLERANCE PROTEIN 9 (OsMTP9), required for manganese (Mn) uptake, are also polarly localized at the distal (OsNramp5) and proximal (OsBOR1 and OsMTP9) sides of the same cell layers (Sasaki et al. 2012; Ueno et al. 2015; Huang et al. 2022). In addition, 3 ammonium transporters (OsAMT1;1, 1;2, and 1;3) also show polar localization at the distal side of exodermis (Konishi and Ma 2021). Since rice roots have aerenchyma in the cortex and 2 Casparian strips (CSs) located at the exodermis and endodermis in its mature region (Enstone et al. 2002), both influx and efflux transporters located at both the exodermis and endodermis are required for the radial transport of mineral elements from soil solution to the root stele (Che et al. 2018; Huang et al. 2024a). For example, Si, as silicic acid, is first imported into the symplast of the exodermal cell by OsLsi1 localized at the distal side of the plasma membrane and then exported by OsLsi2 at the proximal side to the aerenchyma (Ma and Yamaji 2015; Huang and Ma 2024). Si is further imported into the symplast of the endodermis by OsLsi1 localized at the distal side and is exported to the stele by OsLsi2 localized at the proximal side (Ma and Yamaji 2015).

It has been proposed that the polar localization of transporters is important for the directional and efficient uptake of mineral

Received February 5, 2025. Accepted April 18, 2025.

elements (Ma and Yamaji 2015; Yoshinari and Takano 2017; Robe and Barberon 2023). In fact, it was reported that loss of polarity of Nodulin 26-like Intrinsic Protein (NIP) 5;1 (AtNIP5;1), AtBOR1, and AtIRT1 in Arabidopsis caused a significant decrease in the uptake of B and metal ions, respectively (Barberon et al. 2014; Wang et al. 2017; Yoshinari et al. 2019). Recently, it was also found that loss of the polar localization of OsLsi1 resulted in decreased Si uptake in rice (Konishi et al. 2023). However, it is still poorly understood on the role of polar localization of transporters in the uptake of different mineral elements. In the present study, we investigated the role of OsLsi1 polar localization in metalloid uptake in rice. OsLsi1 belongs to the NIP subfamily of aquaporin and was initially identified as a transporter for Si as silicic acid and germanium (Ge), an analog of Si, in rice (Ma et al. 2006). Subsequent studies show that OsLsi1 is also permeable to other metalloids, including B as boric acid (Mitani et al. 2008; Mitani-Ueno et al. 2011; Shao et al. 2018), arsenic (As) as arsenite (Ma et al. 2008), selenium (Se) as selenite (Zhao et al. 2010), and antimony (Sb) as antimonite (Huang et al. 2024b). This is because these metalloids are present in the form of noncharged molecules similar to silicic acid under a pH below 9.0 (Yamaji and Ma 2021). Knockout of *OsLsi1* resulted in decreased accumulation of these metalloids in the shoots (Ma et al. 2008; Zhao et al. 2010; Shao et al. 2018; Huang et al. 2024b); however, the role of OsLsi1 polar localization in the uptake of these metalloids is still unknown. Recently, it was reported that the polar localization of OsLsi1 requires Ile18 at the *N*-terminus, Ile285, and the positively charged cluster at the C-terminus (Konishi et al. 2023). When Ile18 and Ile285 were substituted with Ala, the generated OsLsi1$^{I18A,\ I285A}$ showed nonpolar localization without any reduction of Si/Ge permeability in *Xenopus* oocyte (Konishi et al. 2023). These findings make it possible to investigate the role of OsLsi1 polarity in the uptake of metalloids by comparing plants expressing polar and nonpolar OsLsi1 variants. Through various functional analyses, including gene expression, protein abundance and localization, and phenotypic analysis, we found that the role of polar localization of OsLsi1 in metalloid uptake depends on their species and external concentrations in rice.

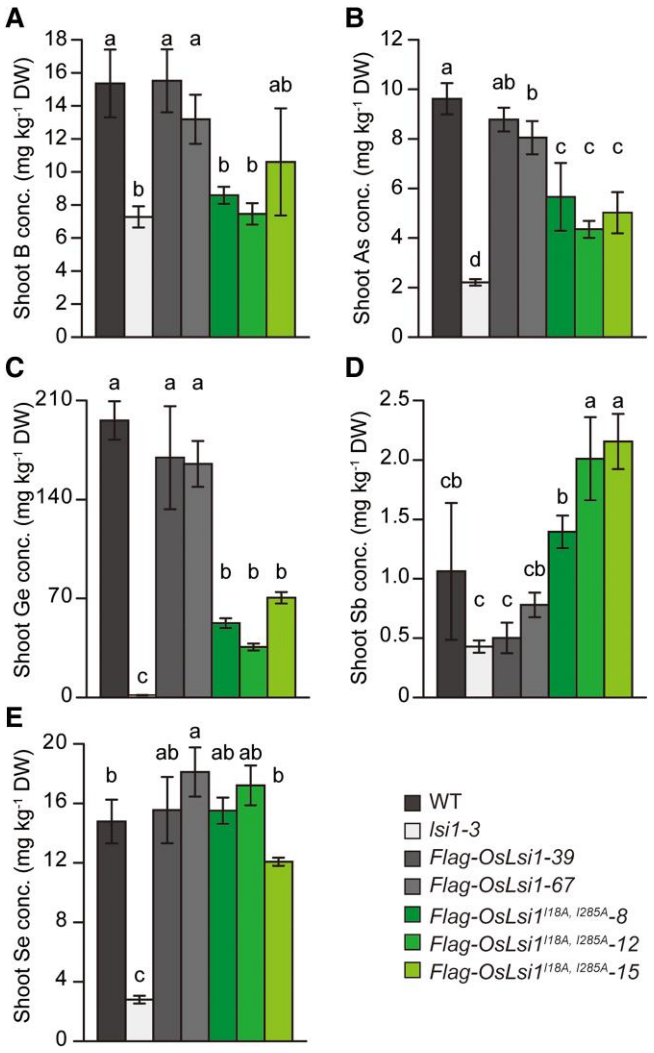

Figure 1. Comparison of shoot metalloid accumulation in plants harboring polar and nonpolar OsLsi1. **A** to **E)** Concentrations of B **A)**, As **B)**, Ge **C)**, Sb **D)**, and Se **E)** in shoots of plants harboring polar and nonpolar OsLsi1. Seedlings (6-d-old) of WT (WT rice), *lsi1-3*, 2 independent *Flag-OsLsi1* transgenic lines, and 3 independent *Flag-OsLsi1*$^{I18A,\ I285A}$ were grown in a hydroponic solution containing 3 μM B for 15 d **A**, **B)** or 12 d **C** to **E)**. Before harvest, the plants were exposed to a solution containing 2 μM of Ge, As, Se, or Sb in the presence of 3 μM B for 24 h. Concentration of metalloids was determined by ICP-MS. Data are means ± SD ($n = 3$ to 4). Different letters indicate significant differences at $P < 0.05$ by Tukey–Kramer's test. DW, dry weight.

Results

Role of OsLsi1 polar localization in metalloid accumulation

We first compared metalloid accumulation in the shoots using transgenic lines harboring polar (*Flag-OsLsi1*) and nonpolar OsLsi1 (*Flag-OsLsi1*$^{I18,\ I285A}$). Introduction of polar OsLsi1 into the *lsi1-3* loss-of-function mutant completely complemented the accumulation of all metalloids tested (Fig. 1, A to E). However, loss of polar localization of OsLsi1 resulted in decreased accumulation of B, As, and Ge in the shoots (Fig. 1, A to C), but increased Sb accumulation at realistic concentrations (2 to 3 μM) (Fig. 1D). The Se accumulation in the shoots was similar between plants with polar and nonpolar OsLsi1 (Fig. 1E).

Role of OsLsi1 polar localization in B uptake at different B concentrations

We further investigated the role of OsLsi1 polar localization in B uptake at different B concentrations. After cultivated for 21 d at low B concentrations (0.3 and 3 μM), the B concentration in the shoots and roots was lower in plants with nonpolar localization than those with polar localization (Fig. 2, A and B). At 30 μM B supply, B concentration in both the roots and shoots showed similar levels in plants with polar and nonpolar localization of OsLsi1 (Fig. 2, A and B). However, at the high B condition (300 μM), the B concentration was increased 2 to 4 times in the shoots of plants with nonpolar localization compared with those with polar localization, whereas it was similar in the roots of plants with polar localization as those with nonpolar localization (Fig. 2, A and B). The B uptake calculated showed a similar trend as shoot B concentration (Fig. 2, A and C). The biomass of the roots and shoots did not differ among different lines at all B concentrations tested (Supplementary Fig. S1, A and B), but the B toxicity symptom (necrosis) was observed in the old leaf (Leaf 4) of plants harboring nonpolar OsLsi1, but not in other lines (Supplementary Fig. S1C). This result is consistent with increased B concentration in the shoots of plants harboring nonpolar OsLsi1 (Fig. 2A).

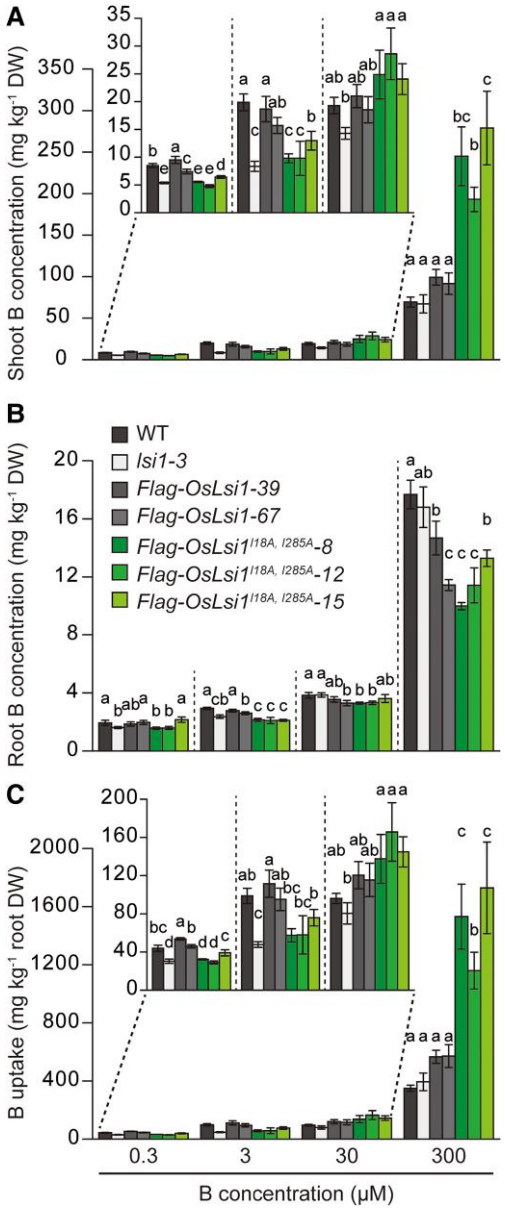

Figure 2. Effect of OsLsi1 polar localization on B uptake at different B concentrations. **A** to **C)** B concentration in the shoots **A)** and roots **B)** and B uptake **C)**. Seedlings (6-d-old) of WT (WT rice), *lsi1*-3, 2 independent *Flag-OsLsi1* transgenic lines, and 3 independent *Flag-OsLsi1*$^{I18A,\ I285A}$ lines were grown in solutions containing 0.3, 3, 30, or 300 μM B for 21 d. Concentration of B in the roots and shoots was determined by ICP-MS. Uptake was calculated by (shoot B content + root B content)/root dry weight. Data are means ± SD ($n = 4$). Different letters indicate a significant difference at $P < 0.05$ by Tukey–Kramer's test. DW, dry weight.

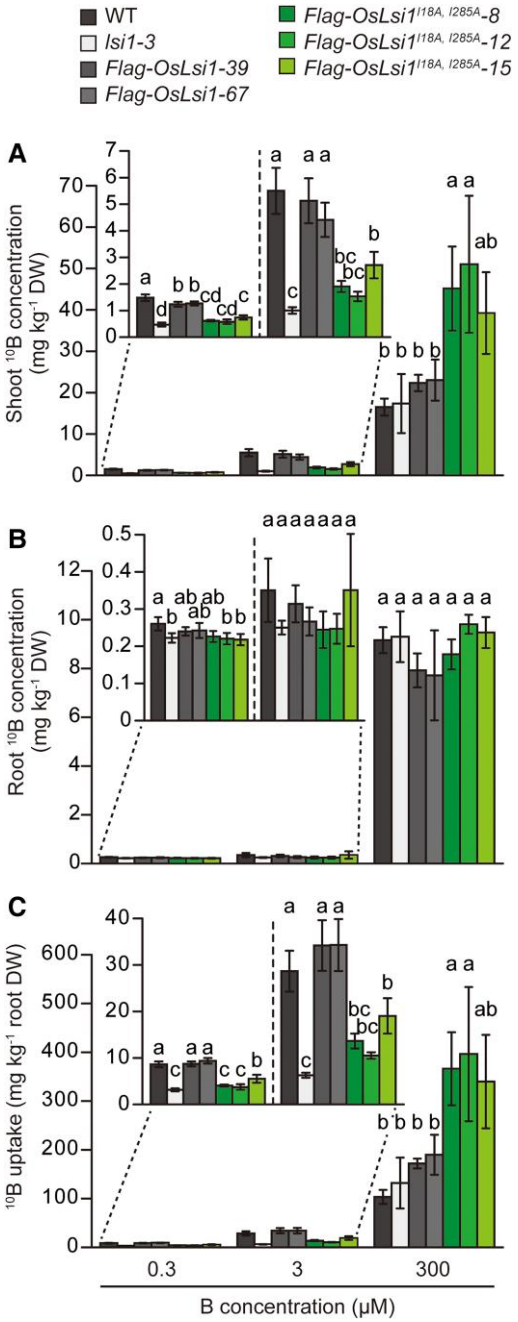

Figure 3. Effect of OsLsi1 polar localization on short-term ^{10}B uptake at different ^{10}B concentrations. **A**, **B)** ^{10}B concentration in the shoots **A)** and roots **B)** and ^{10}B uptake **C)**. Seedlings (6-d-old) of WT (WT rice), *lsi1*-3, 2 independent *Flag-OsLsi1* transgenic lines, and 3 independent *Flag-OsLsi1*$^{I18A,\ I285A}$ lines were precultured in solutions containing 0.3, 3, or 300 μM ^{11}B for 33 d. Before harvest, the plants were exposed to a solution containing 0.3, 3, or 300 μM ^{10}B for 24 h. Concentration of ^{10}B in the roots and shoots was determined by ICP-MS using an isotope model. ^{10}B uptake was calculated by (shoot ^{10}B content + root ^{10}B content)/root dry weight. Data are means ± SD ($n = 4$). Different letters indicate significant differences at $P < 0.05$ by Tukey–Kramer's test. DW, dry weight.

Short-term labeling experiment with ^{10}B

To confirm above results (Fig. 2), we performed a short-term labeling experiment with ^{10}B. To do this, plants were precultured with ^{11}B at 0.3, 3, and 300 μM for 33 d, followed by exposure to a solution containing different concentrations of ^{10}B for 24 h. Similar to the results in Fig. 2, ^{10}B concentration in the shoots was lower in the plants carrying nonpolar OsLsi1 than those carrying polar OsLsi1 at 0.3 and 3 μM ^{10}B (Fig. 3A). However, at 300 μM ^{10}B supply, the shoot ^{10}B concentration was 1.7 to 3 times higher in plants harboring nonpolar OsLsi1 compared with those harboring polar OsLsi1 (Fig. 3A). The roots showed much lower ^{10}B concentration than the shoots, and no difference was found among different lines (Fig. 3B). The calculated ^{10}B uptake showed a similar trend as shoot ^{10}B concentration (Fig. 3, A and C).

Transport activity of polar and nonpolar OsLsi1 for boric acid in *Xenopus* oocyte

To understand the mechanism underlying nonpolar OsLsi1-mediated alteration of B uptake (Figs. 2 and 3), we first compared the transport activity of polar (Flag-OsLsi1) and nonpolar OsLsi1 (Flag-OsLsi1$^{I18A,\ I285A}$) for B, as boric acid, in *Xenopus* oocytes. The result showed that both OsLsi1 variants with polar and nonpolar localization showed B transport activity (Supplementary Fig. S2). Furthermore, the transport activity for boric acid was similar between 2 variants of OsLsi1. This observation indicates that Ala substitutions at Ile18 and Ile285 do not affect the transport activity of OsLsi1 for boric acid.

Effect of polar localization of OsLsi1 on the expression of the transporter genes involved in B uptake

Because uptake of B is mediated by OsLsi1 and OsBOR1 in rice roots, we then compared the expression level of these 2 transporter genes between plants harboring polar and nonpolar OsLsi1 at low (0.3 μM) and high (300 μM) B conditions. The expression level of *OsLsi1* was variable among different transgenic lines, but overall, the expression level was comparable between plants with polar and nonpolar OsLsi1, which was not affected by B concentrations (Fig. 4A). By contrast, the expression level of *OsBOR1* was similar among all lines (Fig. 4B). These results indicate that the altered B uptake in plants with nonpolar localization is not caused by differential gene expression of transporters for B uptake.

Effect of polar localization of OsLsi1 on the B transporters at the protein level under various B concentrations

Since root OsBOR1 protein is degraded in response to high B (Huang et al. 2022), we therefore investigated whether the polar localization of OsLsi1 affects the protein response of OsLsi1 and OsBOR1 to external B concentrations. We selected 2 transgenic lines, *Flag-OsLsi1-67* and *Flag-OsLsi1*$^{I18A,\ I285A}$*-8*, showing similar expression levels (Fig. 4A), and compared the protein abundance of OsLsi1 and OsBOR1 at different B concentrations. The results showed that the abundance of OsLsi1 variants was similar in plants with polar and nonpolar OsLsi1 at all B concentrations tested (Fig. 5A), indicating that both polar and nonpolar OsLsi1 did not respond to high B. By contrast, the protein abundance of OsBOR1 was gradually decreased with increasing B concentrations (Fig. 5B). At 300 μM B, OsBOR1 protein disappeared in both lines (Fig. 5B). However, there was no difference in the protein abundance and response of OsBOR1 to different B concentrations between plants harboring polar and nonpolar OsLsi1 (Fig. 5B). The abundance of H^+-ATPase, as loading control, was comparable in all samples (Fig. 5C).

Effect of polar localization of OsLsi1 on the cellular and subcellular localization of B transporters at different B concentrations

We further performed a double immunostaining of Flag-OsLsi1 and OsBOR1 in transgenic lines at different B concentrations. In the roots of both plants with polar and nonpolar OsLsi1, a Flag signal was observed at root exodermis and endodermis, irrespectively of B concentrations (Fig. 6, A to C). Furthermore, polar localization at the distal side of both cell layers was observed in the roots of plants harboring Flag-OsLsi1, but not in plants harboring the Flag-OsLsi1$^{I18,\ I285}$ (Fig. 6, D to I), confirming our previous

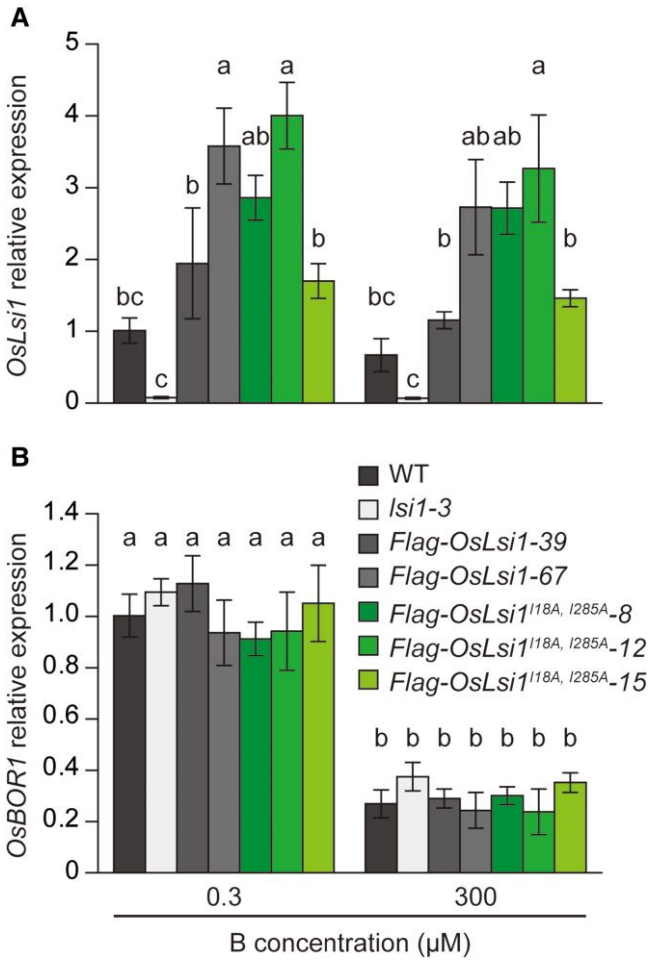

Figure 4. Comparison of expression level of *OsLsi1* and *OsBOR1* in roots of plants expressing polar and nonpolar OsLsi1 at low and high B concentrations. **A**, **B)** Expression level of *OsLsi1* **A)** and *OsBOR1* **B)** in the roots. Seedlings (18-d-old) of WT (WT rice), *lsi1*-3, 2 independent *Flag-OsLsi1* transgenic lines, and 3 independent *Flag-OsLsi1*$^{I18A,\ I285A}$ lines were grown in solutions containing 0.3 or 300 μM B. After 3 d, the roots were sampled for RNA extraction. Expression of *OsLsi1* and *OsBOR1* was determined by reverse transcription quantitative PCR. *HistoneH3* and *Ubiquitin* genes were used as internal controls. Expressions relative to WT at 0.3 μM B are shown. Data are means ± SD ($n = 4$). Different letters indicate significant differences at $P < 0.05$ by Tukey–Kramer's test.

results (Konishi et al. 2023). On the other hand, OsBOR1 signal was mainly observed at the exodermis and endodermis at 0.3 and 3 μM B in the roots of both plants carrying polar and nonpolar *OsLsi1*, but this signal was gradually decreased in response to high B concentrations (Fig. 6, A to C). The polar localization of OsBOR1 at the proximal side was observed in both plants harboring polar and nonpolar OsLsi1 at 0.3 and 3 μM B (Fig. 6, D to I), indicating that loss of polar localization of OsLsi1 did not affect the polar localization of OsBOR1.

Quantitative analysis of signal intensity showed that there was no difference in the signal intensity of Flag-OsLsi1 and OsBOR1 between the plants with polar and nonpolar OsLsi1 at the same B concentration (Fig. 6, J and K). However, in contrast to OsLsi1, which did not respond to B concentrations, the intensity of OsBOR1 decreased with increasing B concentrations in the external solution in both plants with polar and nonpolar OsLsi1 (Fig. 6, J and K).

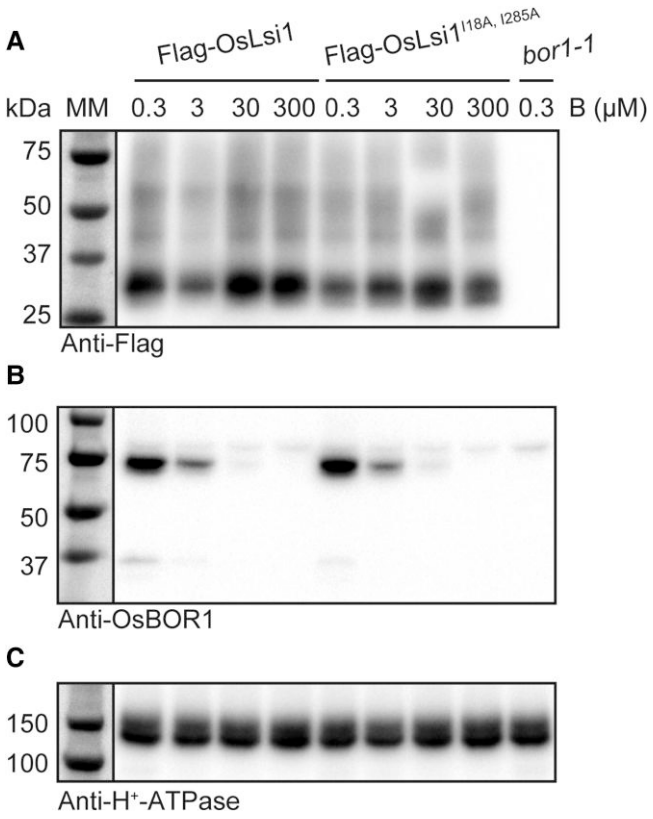

Figure 5. Response of OsLsi1 and OsBOR1 proteins in the roots of plants expressing polar and nonpolar OsLsi1 to different B concentrations. **A** to **C)** Western blotting of Flag-OsLsi1 variants **A)**, OsBOR1 **B)**, and H^+-ATPase **C)**. Seedlings (22-d-old) of transgenic plants carrying *Flag-OsLsi1* (*line67*) and *Flag-OsLsi1*$^{I18A,\ I285A}$ (*line8*) were exposed to a solution containing 0.3, 3, 30, and 300 μM B for 3 d. The knockout mutant of *OsBOR1* (*bor1-1*) treated with 0.3 μM B for 3 d was used as a negative control of Flag and OsBOR1 antibodies. The same amount of protein (7 μg) of microsome fraction was analyzed by SDS-PAGE and visualized by western blot with antibodies against Flag, OsBOR1, and H^+-ATPase (as an internal standard). MM indicates molecular marker.

Discussion

In the present study, by taking advantage of using transgenic plants harboring polar and nonpolar localization of OsLsi1, we were able to investigate the role of its polar localization in the uptake of metalloids. Through various functional analyses, we revealed that the role of polar localization of OsLsi1 in metalloid uptake differs with metalloid species and their concentrations in the external solution.

Metalloid-dependent role of polar localization of OsLsi1 in their uptake

OsLsi1, polarly localized at the distal side of both root exodermis and endodermis, is involved in the uptake of several metalloids, including Ge as germanic acid, B as boric acid, As as arsenite, Sb as antimonite, and Se as selenite, in addition to Si as silicic acid, which are all present in the form of noncharged molecules at a pH below 9 (Yamaji and Ma 2021; Huang et al. 2024b). However, the loss of polar localization of OsLsi1 resulted in decreased (Ge, As, and B), increased (Sb), and unchanged (Se) uptake (Fig. 1). These differences could be attributed to the presence or absence of efflux transporter for these metalloids in the roots. In rice roots, the uptake of mineral elements generally requires both influx and efflux transporters polarly localized at the distal and proximal sides, respectively, of exodermis and endodermis (Che et al. 2018; Huang et al. 2024a; Huang and Ma 2024). Among metalloids tested, similar to Si, the uptake of Ge and As is mediated by OsLsi1 and OsLsi2 (Ma et al. 2006, 2007, 2008), while that of B is mediated by OsLsi1 and OsBOR1 (Nakagawa et al. 2007; Shao et al. 2018; Huang et al. 2022). These polarly localized influx–efflux transporters at the same cells form a directional transport pathway for Si, Ge, As, and B from soil solution to the stele for subsequent translocation to the shoots (Fig. 7A). When polar localization of OsLsi1 is lost, these metalloids effluxed by OsLsi2 or OsBOR1 to the inner apoplastic space will be retaken up by OsLsi1 localized at the proximal side of the exodermis and endodermis because OsLsi1 is bidirectional channel, which transports metalloids following concentration gradient (Mitani et al. 2008) (Fig. 7B). As a result, the efficiency of the uptake for these metalloids is decreased (Fig. 7, A and B).

In contrast to Si, As, and B, the shoot Sb accumulation was increased due to loss of polar localization of OsLsi1 (Fig. 1). In the case of Sb, most Sb taken up by OsLsi1 is retained at the exodermis due to lack of efflux transporter (Fig. 7C; Huang et al. 2024b). However, when polar localization of OsLsi1 is lost, Sb could be effluxed from exodermis to aerenchyma through OsLsi1 localized at the proximal side and further to the stele, resulting in increased Sb accumulation in the shoots (Fig. 7D). On the other hand, loss of polar localization of OsLsi1 does not affect Se accumulation in the shoots (Fig. 1). This is because different from other metalloids, Se taken up by OsLsi1 is readily converted to other organic forms, such as selenomethionine, selenocysteine, and methylselenocysteine in the roots, which are subsequently transported to the shoots by different type of transporters (Zhang et al. 2019).

B concentration-dependent role of polar localization of OsLsi1 in B uptake

Although B functions as an essential element for plants, its range between B deficiency and toxicity is narrower than any other element (Eaton 1944). Therefore, in response to external B fluctuations, plants have developed a fine-tuned system for maintaining optimal internal B levels through the regulation of transporters involved in uptake, root-to-shoot translocation, and distribution (Takano et al. 2010; Kasai et al. 2011; Tanaka et al. 2011, 2016; Yoshinari et al. 2016, 2018, 2021; Aibara et al. 2018; Shao et al. 2018; 2021; Huang et al. 2022). In rice, 2 transporters involved in B uptake show different responses to B fluctuations; OsLsi1 does not respond to external B changes at both transcriptional and translational levels, whereas OsBOR1 is downregulated upon high B concentrations (Figs. 4 and 5; Huang et al. 2022). In the present study, we found that the polar localization of OsLsi1 plays different roles at low and high B concentrations. Under low B concentrations, B uptake was decreased by the loss of OsLsi1 polar localization, whereas at high B concentrations, it was increased in plants with nonpolar OsLsi1 (Figs. 2 and 3). Since there were no differences in B transport activity, localization, protein abundance, and B-dependent response of B transporters between plants harboring polar and nonpolar OsLsi1 variants (Figs. 4 to 6; Supplementary Fig. S2), the B concentration-dependent roles of OsLsi1 polar localization in B uptake seems to be attributed to the presence or absence of OsBOR1. When both OsLsi1 and OsBOR1 are present at low B concentrations, loss of OsLsi1 polar localization decreases the efficiency of B uptake due to the disruption of directional B transport, discussed above (Fig. 7, A and B). However, at high B concentrations, due to the absence of OsBOR1 in both plants with polar and nonpolar OsLsi1 (Fig. 6),

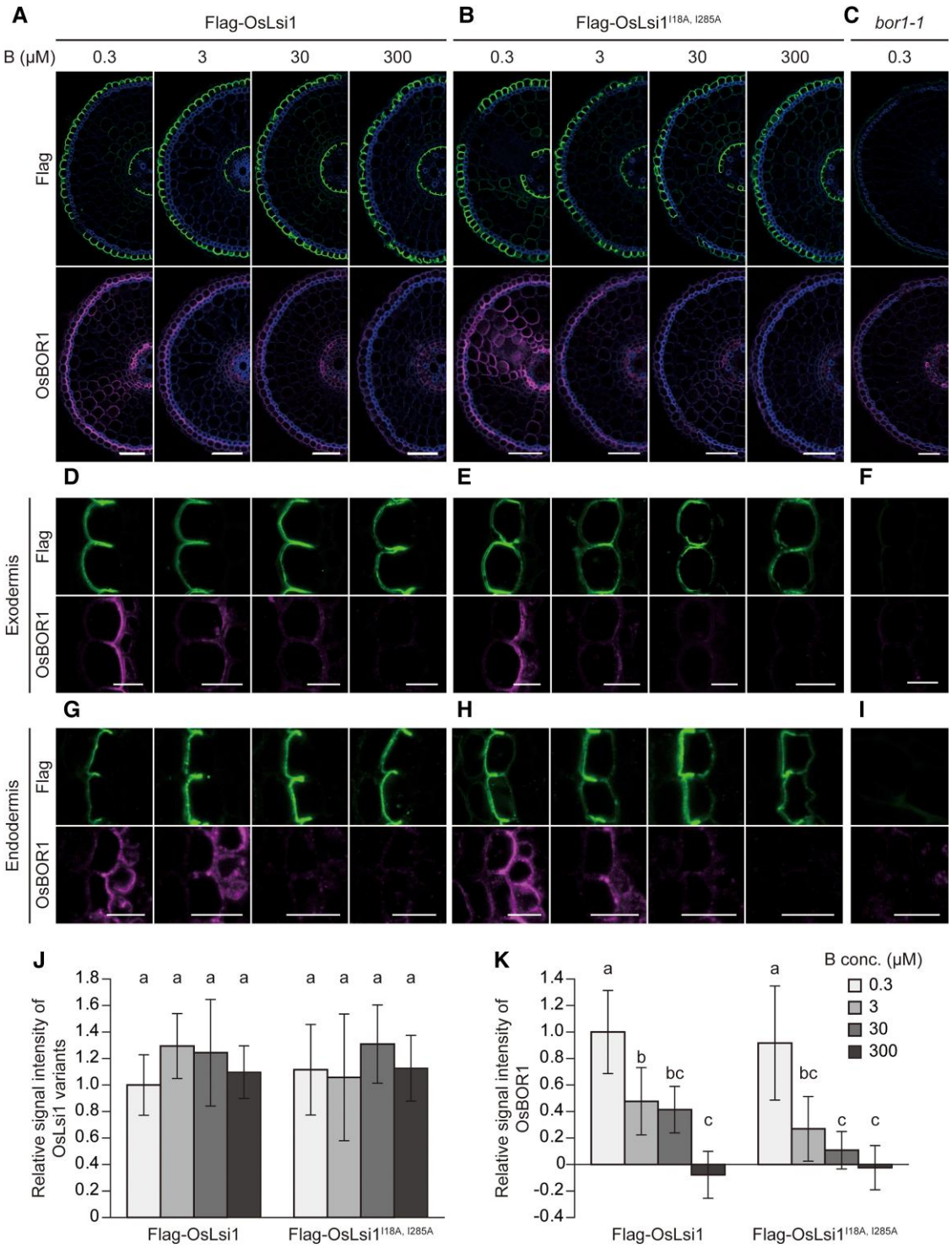

Figure 6. Cellular and subcellular localization of OsLsi1 variants and OsBOR1 at different B concentrations in roots of plants harboring polar and nonpolar OsLsi1. **A** to **C)** Double immunostaining of Flag-OsLsi1 variants (green color, upper panel) and OsBOR1 (magenta color, lower panel) in transgenic plants harboring polar OsLsi1 **A)**, nonpolar OsLsi1 **B)**, and knockout mutant of *OsBOR1* (*bor1-1*) **C)**, as a negative control, at different B concentrations from 0.3 to 300 μM B. **D** to **I)** Enlarged images of Flag-OsLsi1 variants (green color, upper panel) and OsBOR1 (magenta color, lower panel) at exodermis **D** to **F)** and endodermis **G** to **I)** of the roots. Seedlings (28-d-old) of transgenic lines carrying *Flag-OsLsi1* (*line67*) and *Flag-OsLsi1*$^{I18A,\ I285A}$ (*line8*) were exposed to a solution containing 0.3, 3, 30, and 300 μM B for 3 d. The *bor1-1* treated with 0.3 μM B for 3 d was used as a negative control of Flag and OsBOR1 antibodies. Cross-sections of the mature region (10 to 20 mm from the root tip) of the crown root were prepared for immunostaining with Flag and OsBOR1 antibodies, which signals were merged with autofluorescence of the cell wall, indicated by blue color **A** to **C)**. Bars indicate 50 **A** to **C)** or 10 μm **D** to **J)**. Whole root and enlarged images were taken under the same conditions for comparison, respectively. **J**, **K)** Quantified signal intensity of polar and nonpolar OsLsi1 variants **J)** and OsBOR1 **K)**. Signal intensities from Flag and OsBOR1 antibodies of the root images were quantified by LAS AF Lite software **J**, **K)**. The signal of *bor1-1* was subtracted as a background, and signal intensity relative to 0.3 μM B condition was shown **J**, **K)**. Data are means ± SD from 10 independent slices. Different letters indicate significant differences at $P < 0.05$ by Tukey–Kramer's test.

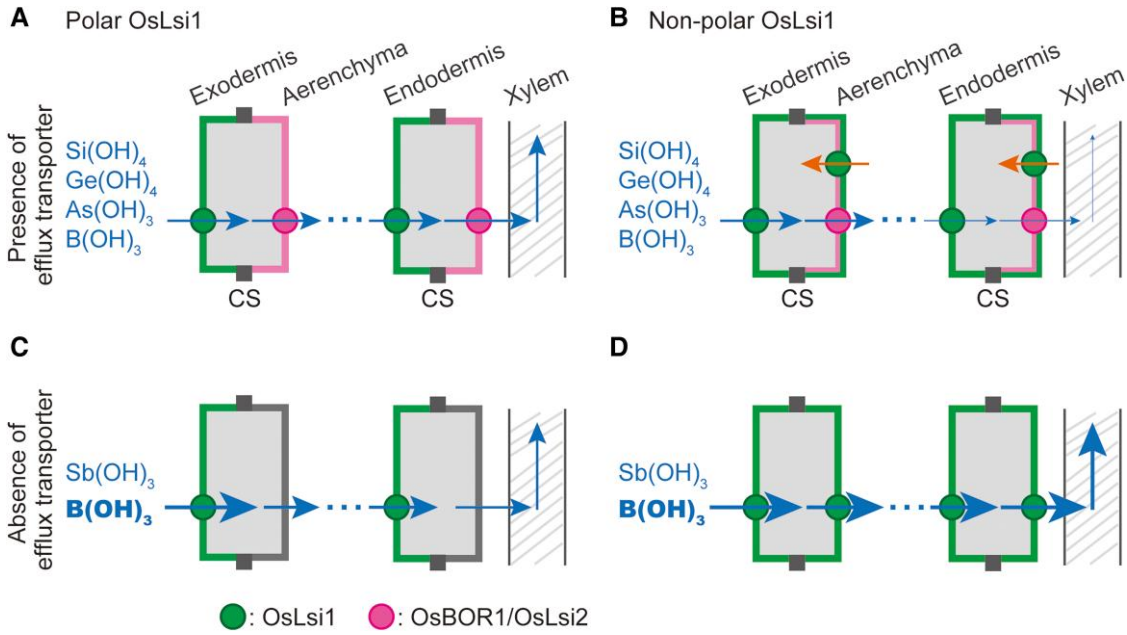

Figure 7. Schematic presentation on the role of OsLsi1 polar localization in metalloid uptake in rice. **A**, **B)** Role of polar localization of OsLsi1 in metalloid uptake in the presence of efflux transporters. When OsLsi1 is polarly localized at the distal side of the exodermis and endodermis **A)**, it forms a directional transport pathway with efflux transporters (OsBOR1 or OsLsi2), facilitating the uptake of metalloids, including B, Si, Ge, and As. However, when OsLsi1 loses its polar localization **B)**, these metalloids effluxed by the efflux transporters to the apoplastic space are retaken up by OsLsi1 localized at the proximal side, decreasing the efficiency of the uptake. **C**, **D)** Role of polar localization of OsLsi1 in metalloid uptake in the absence of efflux transporters. Due to lack of efflux transporter (Sb) or downregulation of OsBOR1 (B at high concentrations), these metalloids taken up by polar OsLsi1 are retained in the exodermal cells, resulting in less root-to-shoot translocation of these metalloids **C)**. However, nonpolar OsLsi1 at the proximal side facilitates the flow of Sb and B toward the stele side **D)**, resulting in increased uptake of these metalloids. Green indicates OsLsi1 localization, while magenta indicates localization of efflux transporters, OsBOR1 and OsBOR2. Blue arrows indicate the flow of metalloids from the soil to the steel, while orange arrows indicate the reuptake of metalloid. CS indicates Casparian strips.

nonpolar OsLsi1 at the proximal side facilitates B permeation through exodermis to the aerenchyma and endodermis to the stele as the case of Sb as discussed above (Fig. 7, C and D). In Arabidopsis, loss of polar localization of AtNIP5;1 also resulted in decreased B uptake at low B concentration (Wang et al. 2017), indicating a common role of polar localization in efficient and directional uptake of B. However, different from OsLsi1 in rice, AtNIP5;1 was downregulated by high B to avoid B toxicity (Tanaka et al. 2011, 2016). Therefore, there is no similar role of polar localization of AtNIP5;1 as observed in rice at high B concentrations (Fig. 7, C and D).

In conclusion, we found that the polar localization of OsLsi1 has different roles in the accumulation of metalloids in the shoots depending on the presence or absence of efflux transporters cooperating with OsLsi1 for each metalloid uptake. Furthermore, we found that its polar localization is not only required for efficient and directional uptake of B at low B concentrations but also required for preventing excess B uptake at high B concentrations in rice roots.

Materials and methods

Plant materials and growth conditions

In the present study, wild-type (WT) rice (*Oryza sativa*. cv. Nipponbare), a loss-of-function mutant of *OsLsi1* (*lsi1-3*; Chiba et al. 2009), a knockout mutant of *OsBOR1* (*bor1-1*; Nakagawa et al. 2007), and transgenic lines carrying *Flag-OsLsi1* with polar localization (2 independent lines) and *Flag-OsLsi1*$^{I18A,\ I285A}$ without polar localization (3 independent lines) in *lsi1-3* background were used. The transgenic lines were generated in our previous studies (Huang et al. 2022; Konishi et al. 2023). Seeds of these lines were soaked in water in the dark at 30°C for 2 d, followed by transferring onto a plastic net floating on a 0.5 mM $CaCl_2$ solution in a 1.2-L plastic pot. After 4 d, the seedlings were transferred to a half-strength Kimura B solution (Ma et al. 2002), containing various B concentrations. The plants were grown in a controlled greenhouse at 25°C to 30°C with natural light. The nutrient solution was changed every 2 d. All experiments were performed with 3 to 4 biological replicates.

Comparison of metalloid accumulation in plants harboring polar and nonpolar OsLsi1

To investigate the role of polar localization of OsLsi1 in uptake of metalloid (B, As, Ge, Sb, and Se), the seedlings (6-d-old) of WT, *lsi1-3*, transgenic plants carrying *Flag-OsLsi1*, and *Flag-OsLsi1*$^{I18A,\ I285A}$ were grown in a half-strength Kimura B solution containing 3 μM boric acid (H_3BO_3) for 15 or 12 d. Before harvest, the seedlings were exposed to a half-strength Kimura B solution, including 3 μM B, containing 2 μM of germanic acid (GeO_2), arsenite ($NaAsO_2$), antimonite ($C_8H_4K_2O12Sb_2{\cdot}3H_2O$), or selenite ($Na_2SeO_3$). After 24 h, the roots were washed with ice-cold 5 mM $CaCl_2$ solution 3 times and separated from the shoots.

To investigate the role of polar localization of OsLsi1 in B uptake at various B concentrations, the seedlings (6-d-old) of WT, *lsi1-3*, transgenic lines were grown in a nutrient solution containing 0.3, 3, 30, or 300 μM B. After growth for 21 d, the roots and shoots were harvested as described above.

Short-term labeling experiment with ^{10}B

We also performed a short-term (24 h) labeling experiment with ^{10}B. To do this, the seedlings (6-d-old) of WT, *lsi1-3*, and transgenic

lines were grown in a nutrient solution containing 0.3, 3, or 300 μM ^{11}B. After growth for 33 d, the plants were washed with a nutrient solution without B for 10 min, followed by exposure to a nutrient solution containing 0.3, 3, or 300 μM ^{10}B, respectively. After 24 h, the roots were washed and separated from the shoots as described above.

Determination of metalloid concentration

All samples harvested in above experiments were dried at 70°C for at least 3 d. Digestion of samples was conducted with HNO_3 (60%) and H_2O_2 (30%) mixture (HNO_3:H_2O_2 = 1:1) at a temperature of up to 110°C in 15-mL plastic tubes (Shao et al. 2018). The concentration of metalloids in the digestion solution was determined by inductively coupled plasma MS (ICP-MS 7700X; Agilent Technologies, Santa Clara, CA, USA). The concentration of ^{10}B and ^{11}B was determined by ICP-MS (8900; Agilent Technologies, Santa Clara, CA, USA) with isotope mode after dilution. B uptake was calculated by (shoot B content + root B content)/root dry weight.

RNA extraction and reverse transcription quantitative PCR analysis

To extract RNA, the roots were sampled from the seedlings (18-d-old) of WT, *lsi1-3*, transgenic plants, which have been exposed to 0.3 and 300 μM B for 3 d. Total RNA was extracted by RNeasy Plus Mini kit (Qiagen) following the manufacturer's instruction. The cDNA was synthesized by ReverTra Ace qPCR RT Master Mix with gDNA Remover (Toyobo). The gene expression level of *OsLsi1* variants and *OsBOR1* in the roots was determined using the KOD SYBR qPCR mix (Toyobo) on a CFX96 system (Bio-Rad) amplified by following primers: 5′-CGGTGGATGTGATCGGAACCA-3′ (forward) and 5′-CGTCGAACT TGTTGCTCGCCA-3′ (reverse) for *OsLsi1* and 5′-CACTAGAAGCCGTGG TGAAA-3′ (forward) and 5′-CAGGTAGTTGCATAGCTCAT-3′ (reverse) for *OsBOR1*. *HistoneH3* and *Ubiquitin* were used as internal standards amplified by following primers 5′-AGTTTGGTCGCTCTCGATTTCG-3′ (forward) and 50-TCAACAAGTTGACCACGTCACG-3′ (reverse) for *HistoneH3* and 5′-GCTCCGTGGCGGTATCAT-3′ (forward) and 5′-CGGCAGTTGACAGCCCTAG-3′ (reverse) for *Ubiquitin*. The relative expression level was calculated using the comparative Ct method.

Western blotting of OsLsi1 variants and OsBOR1

To investigate the protein abundance of B transporters, including OsLsi1 and OsBOR1 in the roots, seedlings (22-d-old) of *bor1-1*, transgenic plants harboring *Flag-OsLsi1* (*line67*), and *Flag-OsLsi1*$^{I18A,\ I285A}$ (*line8*) were exposed to a solution containing 0.3, 3, 30, and 300 μM B. After 3-d exposure, the roots were harvested in ice-cold tubes containing protein extraction buffer (10% glycerol, 5 mM polyvinyl polypyrrolidone, 100 mM Tris-HCl [pH8.0], 5 mM EDTA, 150 mM NaCl, 3.3 mM DTT, and 1 mM phenylmethylsulfonyl fluoride), followed by homogenizing using a Multi-beads shocker (3,000 rpm, 45 s, twice; Yasui Kikai Corporation). Microsome fraction was pelleted by ultracentrifugation according to a previous study (Mitani et al. 2009) and resuspended by resuspension buffer (10% glycerol, 50 mM Tris-HCl [pH8.0], 100 mM sodium phosphate buffer [pH8.0], 5 mM EDTA, 150 mM NaCl, 1% Triton-X100, 3.3 mM DTT, 1 mM phenylmethylsulfonyl fluoride, and 1× protein inhibitor cocktail [Sigma]). The same amounts (7 μg) of microsome protein were subjected to SDS-PAGE using 5% to 20% gradient polyacrylamide gels (e-PAGEL, ATTO, http://www.atto.co.jp) and subsequently to immunoblotting. The membrane was treated with horseradish peroxidase (HRP)-conjugated mouse monoclonal Flag antibody (M2, 1/2,500, Sigma), rabbit polyclonal OsBOR1 antibody (1:1,000 dilutions; Shao et al. 2021), and rabbit polyclonal H^+-ATPase antibody as a control (AS07 260, 1/5,000, Agrisera), respectively. Anti-Rabbit IgG (H + L) HRP Conjugate (1:50,000; Promega, http://www.promega.com) was used as a secondary antibody for OsBOR1 and H^+-ATPase. The ECL Prime Western Blotting Detection Reagent (Cytiva, https://www.cytivalifesciences.co.jp/) was used for detection via chemiluminescence. The signal was captured by a ChemiDoc imager (Bio-Rad).

Double immunostaining of OsLsi1 variants and OsBOR1

Double immunostaining with antibodies against OsBOR1 and Flag for OsLsi1 was performed according to Huang et al. (2022). Cross-sections of crown roots (10 to 20 mm from the tip) were prepared by MicroSlicer (DTK-3000W, Dosaka EM, Co., Ltd.) from seedlings (28-d-old) of transgenic plants carrying *Flag-OsLsi1* (*line67*) and *Flag-OsLsi1*$^{I18A,\ I285A}$ (*line8*), which have been exposed to a solution containing 0.3, 3, 30, and 300 μM B for 3 d. Rat monoclonal Flag (DYKDDDDK) epitope tag antibody (L5, 1/1,000, Novus Biologicals) and the rabbit polyclonal anti-OsBOR1 antibody (1/2,000, Shao et al. 2021) were used, respectively, as a primary antibody. The primary antibody was labeled with Alexa Fluor 488 goat anti-rat IgG for Flag-OsLsi1 variants, while Alexa Fluor 555 goat anti-rabbit IgG for OsBOR1 (Thermo Fisher Scientific). Signals were observed with a confocal laser scanning microscope (TCS SP8X, Leica) with excitation at 555 nm (white light laser) and emission in the range 563 to 580 nm for Alexa Fluor 555, and with excitation at 488 nm (white-light laser) and emission in the range 510 to 560 nm for Alexa Fluor 488. HC PL APO CS2 ×20 dry lens or HC PL APO CS2 ×63 oil immersion lens was used for observations of whole root or enlarged images, respectively. Whole root images and enlarged images were taken under the same conditions, respectively. The signal intensity was quantified by LAS AF Lite software version 4.0 (Leica Microsystems) using 10 independent images. The signal was subtracted from that of *bor1-1* as a background, and signal intensity relative to 0.3 μM B condition was shown.

B transport activity assay in oocytes

Oocytes for transport activity assay were isolated from *Xenopus laevis*. Procedures for deflocculation, culture conditions, and selection were the same as described previously (Mitani et al. 2008). *Flag-OsLsi1* and *Flag-OsLsi1*$^{I18,\ 285A}$ were inserted into the *Xenopus* oocyte expression vector, *pXβG-ev1* (Konishi et al. 2023). Capped RNA was synthesized by in vitro transcription with a mMESSAGE mMACHINE High Yield Capped RNA Transcription Kit (Thermo Fisher Scientific). A volume of 50 nL (1 ng nl^{-1}) cRNA or RNase-free water as a negative control was injected into the oocyte. After cRNA injection and incubated in an MBS for 2 d, the oocytes were transferred to an isotonic solution containing one-fifth diluted MBS supplemented with 175 mM boric acid to adjust the osmolarity. Changes in the oocyte volume were monitored every 20 s up to 180 s. Permeability of boric acid was presented as oocyte volume change [(V V_0^{-1})].

Statistical analysis

ANOVA, followed by Tukey–Kramer's test, was used for comparison using the software BellCurve for Excel (Social Survey Research Information Co., Ltd.).

Accession numbers

Sequence data from this article can be found in the GenBank/EMBL data libraries under accession numbers AB222272 for *OsLsi1* and AK100510 for *OsBOR1*.

Acknowledgments

We thank Akemi Morita, Miho Kashino, and Sanae Rikiishi for their experimental assistance.

Author contributions

N.K. and J.F.M. conceived and designed the experiments. N.K. and N.M.-U. performed the experiments. N.K. analyzed data. N.K. and J.F.M. wrote the manuscript.

Supplementary data

The following materials are available in the online version of this article.

Supplementary Figure S1. Phenotypes of plants expressing polar and nonpolar OsLsi1 at different B concentrations.

Supplementary Figure S2. Boric acid transport activity of polar and nonpolar OsLsi1 variants in *Xenopus* oocytes.

Funding

This work was supported by Japan Society for the Promotion of Science (JSPS) (KAKENHI grant numbers 21H05034 to J.F.M. and 24K17807 to N.K.).

Conflict of interest statement. The authors declare no conflict of interest.

Data availability

The data underlying this article are available in the article and in its online Supplementary Material.

References

Aibara I, Hirai T, Kasai K, Takano J, Onouchi H, Naito S, Fujiwara T, Miwa K. Boron-dependent translational suppression of the borate exporter BOR1 contributes to the avoidance of boron toxicity. *Plant Physiol*. 2018:177(2):759–774. https://doi.org/10.1104/pp.18.00119

Barberon M, Dubeaux G, Kolb C, Isono E, Zelazny E, Vert G. Polarization of IRON-REGULATED TRANSPORTER 1 (IRT1) to the plant-soil interface plays crucial role in metal homeostasis. *Proc Natl Acad Sci U S A*. 2014:111(22):8293–8298. https://doi.org/10.1073/pnas.1402262111

Che J, Yamaji N, Ma JF. Efficient and flexible uptake system for mineral elements in plants. *New Phytol*. 2018:219(2):513–517. https://doi.org/10.1111/nph.15140

Chiba Y, Mitani N, Yamaji N, Ma JF. Hvlsi1 is a silicon influx transporter in barley. *Plant J*. 2009:57(5):810–818. https://doi.org/10.1111/j.1365-313X.2008.03728.x

Eaton FM. Deficiency, toxicity and accumulation of boron in plants. *J Agric Res*. 1944:69:237–279.

Enstone DE, Peterson CA, Ma F. Root endodermis and exodermis: structure, function, and responses to the environment. *J Plant Growth Regul*. 2002:21:335–351.

Gordon-Weeks R, Tong Y, Davies TE, Leggewie G. Restricted spatial expression of a high-affinity phosphate transporter in potato roots. *J Cell Sci*. 2003:116(15):3135–3144. https://doi.org/10.1242/jcs.00615

Guo Z, Cao H, Zhao J, Bai S, Peng W, Li J, Sun L, Chen L, Lin Z, Shi C, *et al*. A natural uORF variant confers phosphorus acquisition diversity in soybean. *Nat Commun*. 2022:13(1):3796. https://doi.org/10.1038/s41467-022-31555-2

Huang H, Yamaji N, Ma JF. Tissue-specific deposition, speciation and transport of antimony in rice. *Plant Physiol*. 2024b:195(4):2683–2693. https://doi.org/10.1093/plphys/kiae289

Huang S, Konishi N, Yamaji N, Shao JF, Mitani-Ueno N, Ma JF. Boron uptake in rice is regulated post-translationally via a clathrin-independent pathway. *Plant Physiol*. 2022:188(3):1649–1664. https://doi.org/10.1093/plphys/kiab575

Huang S, Ma JF. Silicon transport and its "homeostasis" in rice. *Quant Plant Biol*. 2024:5:e15. https://doi.org/10.1017/qpb.2024.19

Huang S, Wang P, Yamaji N, Ma JF. Plant nutrition for human nutrition: hints from rice research and future perspectives. *Mol Plant*. 2020:13(6):825–835. https://doi.org/10.1016/j.molp.2020.05.007

Huang S, Yamaji N, Ma JF. Metal transport systems in plants. *Annu Rev Plant Biol*. 2024a:75(1):1–25. https://doi.org/10.1146/annurev-arplant-062923-021424

Kasai K, Takano J, Miwa K, Toyoda A, Fujiwara T. High boron-induced ubiquitination regulates vacuolar sorting of the BOR1 borate transporter in *Arabidopsis thaliana*. *J Biol Chem*. 2011:286(8):6175–6183. https://doi.org/10.1074/jbc.M110.184929

Kiba T, Feria-Bourrellier AB, Lafouge F, Lezhneva L, Boutet-Mercey S, Orsel M, Bréhaut V, Miller A, Daniel-Vedele F, Sakakibara H, *et al*. The *Arabidopsis* nitrate transporter NRT2.4 plays a double role in roots and shoots of nitrogen-starved plants. *Plant Cell*. 2012:24(1):245–258. https://doi.org/10.1105/tpc.111.092221

Konishi N, Ma JF. Three polarly localized ammonium transporter 1 members are cooperatively responsible for ammonium uptake in rice under low ammonium condition. *New Phytol*. 2021:232(4):1778–1792. https://doi.org/10.1111/nph.17679

Konishi N, Mitani-Ueno N, Yamaji N, Ma JF. Polar localization of a rice silicon transporter requires isoleucine at both C-and N-termini as well as positively charged residues. *Plant Cell*. 2023:35(6):2232–2250. https://doi.org/10.1093/plcell/koad073

Ma JF, Tamai K, Ichii M, Wu GF. A rice mutant defective in Si uptake. *Plant Physiol*. 2002:130(4):2111–2117. https://doi.org/10.1104/pp.010348

Ma JF, Tamai K, Yamaji N, Mitani N, Konishi S, Katsuhara M, Ishiguro M, Murata Y, Yano M. A silicon transporter in rice. *Nature*. 2006:440(7084):688–691. https://doi.org/10.1038/nature04590

Ma JF, Yamaji N. A cooperative system of silicon transport in plants. *Trends Plant Sci*. 2015:20(7):435–442. https://doi.org/10.1016/j.tplants.2015.04.007

Ma JF, Yamaji N, Mitani N, Tamai K, Konishi S, Fujiwara T, Katsuhara M, Yano M. An efflux transporter of silicon in rice. *Nature*. 2007:448(7150):209–212. https://doi.org/10.1038/nature05964

Ma JF, Yamaji N, Mitani N, Xu XY, Su YH, McGrath SP, Zhao FJ. Transporters of arsenite in rice and their role in arsenic accumulation in rice grain. *Proc Natl Acad Sci U S A*. 2008:105(29):9931–9935. https://doi.org/10.1073/pnas.0802361105

Mitani N, Yamaji N, Ma JF. Characterization of substrate specificity of a rice silicon transporter, Lsi1. *Pflug Arch Eur J Phy*. 2008:456(4):679–686. https://doi.org/10.1007/s00424-007-0408-y

Mitani N, Yamaji N, Ma JF. Identification of maize silicon influx transporters. *Plant Cell Physiol*. 2009:50(1):5–12. https://doi.org/10.1093/pcp/pcn110

Mitani-Ueno N, Yamaji N, Zhao FJ, Ma JF. The aromatic/arginine selectivity filter of NIP aquaporins plays a critical role in substrate

selectivity for silicon, boron, and arsenic. *J Exp Bot*. 2011:62(12):4391–4398. https://doi.org/10.1093/jxb/err158

Nakagawa Y, Hanaoka H, Kobayashi M, Miyoshi K, Miwa K, Fujiwara T. Cell-type specificity of the expression of *OsBOR1*, a rice efflux boron transporter gene, is regulated in response to boron availability for efficient boron uptake and xylem loading. *Plant Cell*. 2007:19(8):2624–2635. https://doi.org/10.1105/tpc.106.049015

Rengel Z, Cakmak I, White PJ, editors. *Marschner's mineral nutrition of plants*. Amsterdam, Netherlands: Elsevier; 2022.

Robe K, Barberon M. Nutrient carriers at the heart of plant nutrition and sensing. *Curr Opin Plant Biol*. 2023:74:102376. https://doi.org/10.1016/j.pbi.2023.102376

Sasaki A, Yamaji N, Yokosho K, Ma JF. Nramp5 is a major transporter responsible for manganese and cadmium uptake in rice. *Plant Cell*. 2012:24(5):2155–2167. https://doi.org/10.1105/tpc.112.096925

Shao JF, Yamaji N, Huang S, Ma JF. Fine regulation system for distribution of boron to different tissues in rice. *New Phytol*. 2021:230(2):656–668. https://doi.org/10.1111/nph.17169

Shao JF, Yamaji N, Liu XW, Yokosho K, Shen RF, Ma JF. Preferential distribution of boron to developing tissues is mediated by the intrinsic protein OsNIP3. *Plant Physiol*. 2018:176(2):1739–1750. https://doi.org/10.1104/pp.17.01641

Takano J, Tanaka M, Toyoda A, Miwa K, Kasai K, Fuji K, Onouchi H, Naito S, Fujiwara T. Polar localization and degradation of *Arabidopsis* boron transporters through distinct trafficking pathways. *Proc Natl Acad Sci U S A*. 2010:107(11):5220–5225. https://doi.org/10.1073/pnas.0910744107

Tanaka M, Sotta N, Yamazumi Y, Yamashita Y, Miwa K, Murota K, Chiba Y, Hirai MY, Akiyama T, Onouchi H, *et al*. The minimum open reading frame, AUG-stop, induces boron-dependent ribosome stalling and mRNA degradation. *Plant Cell*. 2016:28(11):2830–2849. https://doi.org/10.1105/tpc.16.00481

Tanaka M, Takano J, Chiba Y, Lombardo F, Ogasawara Y, Onouchi H, Naito S, Fujiwara T. Boron-dependent degradation of *NIP5;1* mRNA for acclimation to excess boron conditions in *Arabidopsis*. *Plant Cell*. 2011:23(9):3547–3559. https://doi.org/10.1105/tpc.111.088351

Ueno D, Sasaki A, Yamaji N, Miyaji T, Fujii Y, Takemoto Y, Moriyama S, Che J, Moriyama Y, Iwasaki K, *et al*. A polarly localized transporter for efficient manganese uptake in rice. *Nat Plant*. 2015:1(12):1–8. https://doi.org/10.1038/nplants.2015.170

Ueno D, Yamaji N, Ma JF. Further characterization of ferric-phytosiderophore transporters ZmYS1 and HvYS1 in maize and barley. *J Exp Bot*. 2009:60(12):3513–3520. https://doi.org/10.1093/jxb/erp191

Wang S, Yoshinari A, Shimada T, Hara-Nishimura I, Mitani-Ueno N, Ma JF, Naito S, Takano J. Polar localization of the NIP5;1 boric acid channel is maintained by endocytosis and facilitates boron transport in *Arabidopsis* roots. *Plant Cell*. 2017:29(4):824–842. https://doi.org/10.1105/tpc.16.00825

Yamaji N, Ma JF. Metalloid transporters and their regulation in plants. *Plant Physiol*. 2021:187(4):1929–1939. https://doi.org/10.1093/plphys/kiab326

Yoshinari A, Fujimoto M, Ueda T, Inada N, Naito S, Takano J. DRP1-dependent endocytosis is essential for polar localization and boron-induced degradation of the borate transporter BOR1 in *Arabidopsis thaliana*. *Plant and Cell Physiol*. 2016:57(9):1985–2000. https://doi.org/10.1093/pcp/pcw121

Yoshinari A, Hosokawa T, Amano T, Beier MP, Kunieda T, Shimada T, Hara-Nishimura I, Naito S, Takano J. Polar localization of the borate exporter BOR1 requires AP2-dependent endocytosis. *Plant Physiol*. 2019:179(4):1569–1580. https://doi.org/10.1104/pp.18.01017

Yoshinari A, Hosokawa T, Beier MP, Oshima K, Ogino Y, Hori C, Takasuka TE, Fukao Y, Fujiwara T, Takano J. Transport-coupled ubiquitination of the borate transporter BOR1 for its boron-dependent degradation. *Plant Cell*. 2021:33(2):420–438. https://doi.org/10.1093/plcell/koaa020

Yoshinari A, Korbei B, Takano J. TOL proteins mediate vacuolar sorting of the borate transporter BOR1 in *Arabidopsis thaliana*. *Soil Sci Plant Nutr*. 2018:64(5):598–605. https://doi.org/10.1080/00380768.2018.1504322

Yoshinari A, Takano J. Insights into the mechanisms underlying boron homeostasis in plants. *Front Plant Sci*. 2017:8:1951. https://doi.org/10.3389/fpls.2017.01951

Zhang L, Hu B, Deng K, Gao X, Sun G, Zhang Z, Li P, Wang W, Li H, Zhang Z, *et al*. NRT1.1B improves selenium concentrations in rice grains by facilitating selenomethinone translocation. *Plant Biotechnol J*. 2019:17(6):1058–1068. https://doi.org/10.1111/pbi.13037

Zhao XQ, Mitani N, Yamaji N, Shen RF, Ma JF. Involvement of silicon influx transporter OsNIP2;1 in selenite uptake in rice. *Plant Physiol*. 2010:153(4):1871–1877. https://doi.org/10.1104/pp.110.157867